

“Treasure maps” for magnetic high-entropy-alloys from theory and experiment

F. Körmann, D. Ma, D. D. Belyea, M. S. Lucas, C. W. Miller, B. Grabowski, and M. H. F. Sluiter

Citation: [Applied Physics Letters](#) **107**, 142404 (2015); doi: 10.1063/1.4932571

View online: <http://dx.doi.org/10.1063/1.4932571>

View Table of Contents: <http://scitation.aip.org/content/aip/journal/apl/107/14?ver=pdfcov>

Published by the [AIP Publishing](#)

Articles you may be interested in

[Thermomagnetic analysis of FeCoCr x Ni alloys: Magnetic entropy of high-entropy alloys](#)

J. Appl. Phys. **113**, 17A923 (2013); 10.1063/1.4798340

[Effects of alloying elements and temperature on the elastic properties of dilute Ni-base superalloys from first-principles calculations](#)

J. Appl. Phys. **112**, 053515 (2012); 10.1063/1.4749406

[Alloying effects on the elastic parameters of ferromagnetic and paramagnetic Fe from first-principles theory](#)

J. Appl. Phys. **110**, 073707 (2011); 10.1063/1.3644907

[Magnetic and vibrational properties of high-entropy alloys](#)

J. Appl. Phys. **109**, 07E307 (2011); 10.1063/1.3538936

[Magnetic and thermal characteristics of a magnetic shape memory alloy \(Fe–Cr–Ni–Mn–Si–Co\)](#)

J. Appl. Phys. **91**, 7448 (2002); 10.1063/1.1448304

The logo for AIP APL Photonics is displayed on a red background with a bright yellow sunburst effect. The letters 'AIP' are in a large, white, sans-serif font, followed by a vertical bar and the words 'APL Photonics' in a smaller, white, sans-serif font.

AIP | APL Photonics

APL Photonics is pleased to announce
Benjamin Eggleton as its Editor-in-Chief



“Treasure maps” for magnetic high-entropy-alloys from theory and experiment

F. Körmann,^{1,a)} D. Ma,² D. D. Belyea,³ M. S. Lucas,⁴ C. W. Miller,^{5,b)} B. Grabowski,² and M. H. F. Sluiter¹

¹Department of Materials Science and Engineering, Delft University of Technology, Mekelweg 2, 2628 CD Delft, The Netherlands

²Max-Planck-Institut für Eisenforschung GmbH, D-40237 Düsseldorf, Germany

³Department of Physics, University of South Florida, 4202 East Fowler Ave., Tampa, Florida 33620, USA

⁴Air Force Research Laboratory, Wright-Patterson AFB, Ohio 45433, USA

⁵School of Chemistry and Materials Science, Rochester Institute of Technology, 85 Lomb Memorial Drive, Rochester, New York 14623, USA

(Received 22 July 2015; accepted 21 September 2015; published online 6 October 2015)

The critical temperature and saturation magnetization for four- and five-component FCC transition metal alloys are predicted using a formalism that combines density functional theory and a magnetic mean-field model. Our theoretical results are in excellent agreement with experimental data presented in both this work and in the literature. The generality and power of this approach allow us to computationally design alloys with well-defined magnetic properties. Among other alloys, the method is applied to CoCrFeNiPd alloys, which have attracted attention recently for potential magnetic applications. The computational framework is able to predict the experimentally measured T_C and to explore the dominant mechanisms for alloying trends with Pd. A wide range of ferromagnetic properties and Curie temperatures near room temperature in hitherto unexplored alloys is predicted in which Pd is replaced in varying degrees by, e.g., Ag, Au, and Cu. © 2015 AIP Publishing LLC. [<http://dx.doi.org/10.1063/1.4932571>]

Since the revival of multi-principal element alloys more than ten years ago, hundreds of different high entropy alloys (HEAs) have been discovered.¹ Among them are CoCrFeNi-based alloys such as CoCrFeNiMn and CoCrFeNiPd revealing superior mechanical² and promising magnetic properties,^{3,4} respectively. Among other materials,⁵ the latter have been investigated as potential candidates for next-generation magnetic refrigeration applications.⁴ For that purpose, a Curie temperature, T_C , close to room temperature is required which, unfortunately, is not fulfilled for CoCrFeNi alloys with T_C near 100 K.¹ Experiments indicate that additional alloying can change T_C by several hundreds Kelvin, e.g., from 90 K for CoCrFeNiAl_{0.25} up to more than 500 K for CoCrFeNiPd₂ alloys (see Fig. 1).^{3,6} Considering however the immense configurational space of these alloys, the optimization of T_C into a narrow window close to room temperature—under the constraint of preserving other desirable properties—is a highly non-trivial task.

In the present letter, we report predictions for both the critical temperature and saturation magnetization of 4- and 5-component transition metal alloys. As envisioned by the Materials Genome Initiative, this work represents an experimentally validated computational guide for the discovery and design of materials with specifically desired properties. We combine density-functional theory (DFT) with a mean field (MF) magnetic model allowing efficient T_C predictions. The predictive power of this theory is validated with experimental data from a variety of CoFeNi-based HEAs. Our approach allows us to screen a wide compositional range of

HEAs, which essentially provides “treasure maps” of the enormous and unexplored parameter space occupied by four and five component alloys.

Within the last decade, DFT based predictions of finite-temperature magnetic properties, such as Curie temperatures, have become an attractive tool in materials science.^{7–22} One of the most common approaches is to map the DFT energetics onto an effective Heisenberg-like Hamiltonian, $\mathcal{H} = \sum_{ij} J_{ij} \vec{m}_i \cdot \vec{m}_j$.^{7–14} Here, J_{ij} denotes the magnetic exchange interaction between atomic sites i and j with local magnetic moments \vec{m}_i and \vec{m}_j . The Hamiltonian is usually solved via analytic methods^{7–10} or Monte Carlo simulations.^{11–14} In addition to elemental ferromagnets Fe, Co, and Ni,^{8–13} such an approach has been applied to a variety of magnetic materials such as, e.g., FeCo alloys,^{11,22} Heusler alloys,¹⁶ or diluted magnetic semiconductors.^{17–21}

A good approximation to the solution of the Heisenberg Hamiltonian is obtained from a MF approach analogous to the Weiss molecular field theory. Within MF, T_C is directly related to the sum of the magnetic interactions. For elemental ferromagnets such as Fe, Co, or Ni, one obtains $k_B T_C = 2/3 \sum_{ij} \tilde{J}_{ij}$ (see, e.g., Ref. 8), where the local moments are usually absorbed into effective interactions $\tilde{J}_{ij} = J_{ij} m_i m_j$. In practical applications, it is convenient to identify T_C as the energy difference ΔE of the ferromagnetic, E_{FM} , and paramagnetic energy, E_{PM} , of the system as $k_B T_C = 2\Delta E/3$ employing $\sum_{ij} \tilde{J}_{ij} = E_{FM} - E_{PM}$. If alloyed with a small concentration, c , of nonmagnetic elements, T_C reads²¹

$$k_B T_C = \frac{2}{3(1-c)} (E_{FM} - E_{PM}) = \frac{2}{3(1-c)} \Delta E. \quad (1)$$

^{a)}Electronic mail: f.h.w.kormann@tudelft.nl

^{b)}Electronic mail: cwmsch@rit.edu

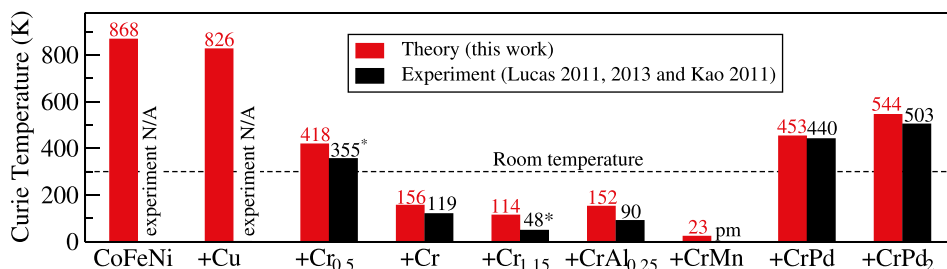


FIG. 1. Theoretical (red bars) and experimental (black bars) Curie temperatures for various CoFeNi-based HEAs. The T_C 's marked with the star have been derived from an empirical linear interpolation.⁴

This concentration dependent MF formulation for T_C has been shown to provide accurate results for a number of systems, e.g., for a variety of diluted magnetic semiconductors.^{17–21} Note, however, that Eq. (1) is not applicable if percolation effects dominate the ferromagnetic ordering, e.g., in the presence of short-ranged magnetic interactions and low magnetic alloying element concentrations ($\approx 20\%$) (see, e.g., Ref. 23).

To compute the ferromagnetic and paramagnetic total energies, we employed the exact muffin-tin orbital-coherent potential approximation (EMTO-CPA) method²⁴ within the generalized gradient approximation.²⁵ The EMTO-CPA approach allows to model solid-solutions within an effective 1-atom unit cell at the cost of neglecting local lattice distortions or local chemical order. This allows us to address an existing difficulty in first-principles modeling of HEAs, in particular with treating their multi-element character with supercell based techniques. Recent DFT studies on HEAs have explored the performance of mean-field type simplifications of the electronic structure problem, such as the CPA,²⁶ as implemented, e.g., in the EMTO method. A further advantage is the possibility to straightforwardly model the paramagnetic state and hence to directly access E_{PM} via the disordered local moment (DLM) approach.²⁷ The DLM resembles a random spin configuration with zero averaged magnetization, while allowing the presence of finite local magnetic moments on each lattice site. EMTO-CPA calculations for HEAs have been carried out to investigate, e.g., phase stabilities and bulk properties^{28–34} as well as stacking fault energies.^{35,36} For CoCrFeNi based HEAs, Tian *et al.* and Niu *et al.* have shown that bulk properties, e.g., bulk moduli²⁸ and enthalpies of formation,³⁴ are in reasonable agreement between CPA and explicit super cell calculations.

The Brillouin zone integration in the FCC alloys was carried out on a $25 \times 25 \times 25$ k -point mesh according to the Monkhorst-Pack scheme.³⁷ Other EMTO parameters were chosen as in Ref. 29. The magnetic energies of the considered multi-component HEAs were mapped onto an effective one-atomic magnetic species alloyed with a nonmagnetic element of concentration c . The energy difference entering Eq. (1) was obtained at the equilibrium volume of the ferromagnetic ground state of the respective alloy. For compositions including Cr, we considered a ferri-magnetic state instead of a ferromagnetic one in line with results from Niu *et al.*³⁴ Ag, Al, Au, Cu, and Pd were treated as nonmagnetic alloying elements in Eq. (1) due to their small induced magnetic moments ($< 0.1\mu_B$).

To verify the performance of our approach, we computed T_C for a number of different alloys for which T_C values have been reported in literature (black and red bars in Fig. 1). As is well-known, the MF approximation

consistently overestimates T_C .¹⁰ Nevertheless, the trend in the measured T_C 's is in very good agreement with our theoretical results indicating the predictive strength of the approach. Further validation with respect to our own measurements is given below.

In order to systematically understand and explore the alloying trends of T_C , we first consider the 3-component CoFeNi alloy. The prediction of $T_C \approx 868$ K (left hand side of Fig. 1) obtained with our approach is not surprising taking into account that all three individual elements are ferromagnetic with a considerable individual T_C (1394 K, 1041 K, and 611 K). The critical temperature does not change much if alloyed with Cu whereas it drops significantly if alloyed with Cr. For the equi-atomic CrCoFeNi HEA, a T_C is found below room temperature consistent with the experimental observations. T_C decreases even further if in addition to Cr the HEA is alloyed with Al or Mn. However, in agreement with experiment, T_C near and above room temperature for CoCrFeNi alloys are found by decreasing the Cr concentration (closer to CoFeNi) or by additional alloying with Pd.

The analysis indicates two possible alloying strategies to achieve room temperature T_C (i) by varying the Cr-content or (ii) by adding additional Pd. We therefore examine in the following more closely under which alloying compositions the transition occurs. Fig. 2(a) shows the impact on T_C by alloying with Pd. Our theoretical data are compared with two previous experimental data points by Lucas *et al.* (black symbols).^{3,4} For CoCrFeNiPd _{x} , we predict a nonlinear dependence of T_C on Pd content in which a strong response regime for small x leads to a weaker dependence above $x = 1$. Analyzing the theoretical data in more detail, we find that these limiting regimes are correlated with the stabilization of Cr magnetic moments in the paramagnetic state (see dashed lines in Fig. 2(a)). This stabilization is driven by the increase in volume due to larger Pd concentrations. The same trend, i.e., a steeper slope of $T_C(c)$ for small Pd concentrations, is observed for other fixed Cr-concentrations, e.g., for CoCr_{0.5}FeNiPd _{x} alloys (orange lines in Fig. 2).

Our theoretical predictions were tested by fabricating and measuring the magnetic properties of six compositions of CoCrFeNiPd _{x} ranging from $x = 0$ to 0.5. Samples were prepared by arc melting in an argon atmosphere using metals with purity 99.99% or greater. The samples were cold rolled into sheets and diced to form ribbons $2\text{ mm} \times 3\text{ mm}$ with thickness of 100 to 250 μm . The samples were then wrapped in Ta foil, sealed in a quartz tube with Ar gas, and annealed for 1 h at 900 $^\circ\text{C}$. Magnetization measurements were made using a Quantum Design Physical Property Measurement System with a vibrating sample magnetometer. Figure 2(a) shows the T_C (red stars), as determined from the modified

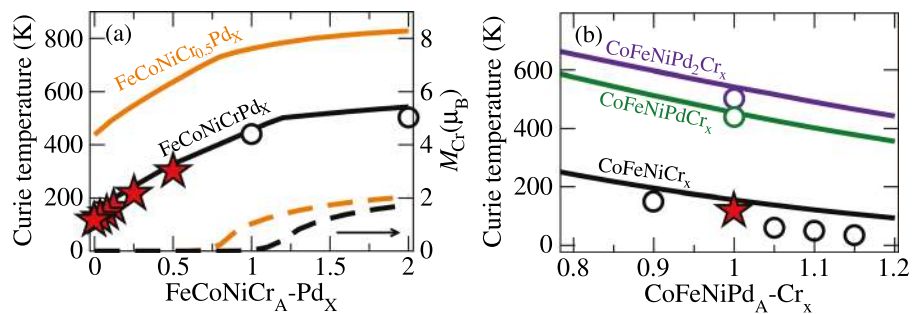


FIG. 2. Theoretical (lines) and experimental (symbols) Curie temperature T_C (a) as a function of Pd concentration for fixed Cr-concentrations including our experimental data (red stars) and (b) as a function of Cr concentration for fixed Pd-concentrations. (a) also shows the stabilization of local magnetic Cr moments in the paramagnetic state (dashed lines) being responsible for the two slopes in T_C . All alloys correspond to a stoichiometric ratio. Open circles mark previous experimental data from Refs. 3 and 4.

Arrott plot technique.³⁸ These data are in excellent agreement with the theoretical predictions, including the theoretically predicted slopes of T_C with Pd content. Further, room temperature X-ray diffraction measurements reveal that the impact of Pd is indeed to increase the lattice parameter, in agreement with the theoretical analysis.³

Previously, Lucas *et al.* have studied the peak position of magnetic entropy change on varying Cr concentration in CoFeNiCr_x alloys.⁴ Their data are also shown in Fig. 2 and compared with our theoretical predictions. The overall agreement is similarly good as for varying the Pd-concentrations, although the theoretical dependence of T_C on Cr-concentration is slightly weaker as observed in experiment.

Having verified that our theoretical approach shows good agreement not only for different alloying elements (Fig. 1) but even for subtle concentration dependent alloying trends (Fig. 2), we explore in the following several T_C alloying phase diagrams which have not been experimentally addressed so far. We first consider the T_C map for CoCrFeNiPd alloys (third column in Fig. 3). The open symbols indicate the previously experimentally accessed cross-sections for varying Cr

and Pd concentrations. The stars indicate our experimental results. The comparison between experiment and theory clearly shows that so far only a very narrow regime of the whole T_C phase space has been explored. The full computed theoretical map goes significantly beyond the previous findings, in that it gives an estimate of the necessary Pd concentration for a given Cr concentration that will result in an alloy whose Curie point is at or near room temperature.

Our theoretical method is not restricted to Pd-containing systems. Indeed, we are able to extend the theory to several additional elements in order to help identify alloys that may have desirable ferromagnetic properties, but which have not yet been experimentally fabricated and tested. As in the Cr-Pd scenario, the T_C maps for FCC Ag, Au, and Cu in combination with Cr have been computed for AgCoCrNiFe, AuCoCrNiFe, and CoCrCuNiFe. As shown in Fig. 3, Curie temperatures close to room temperature are predicted to be possible for all considered HEA combinations under the given compositional dependence. Linear fits to the composition maps' 300 K contours lead to simple equations that indicate the family of alloy compositions for which room

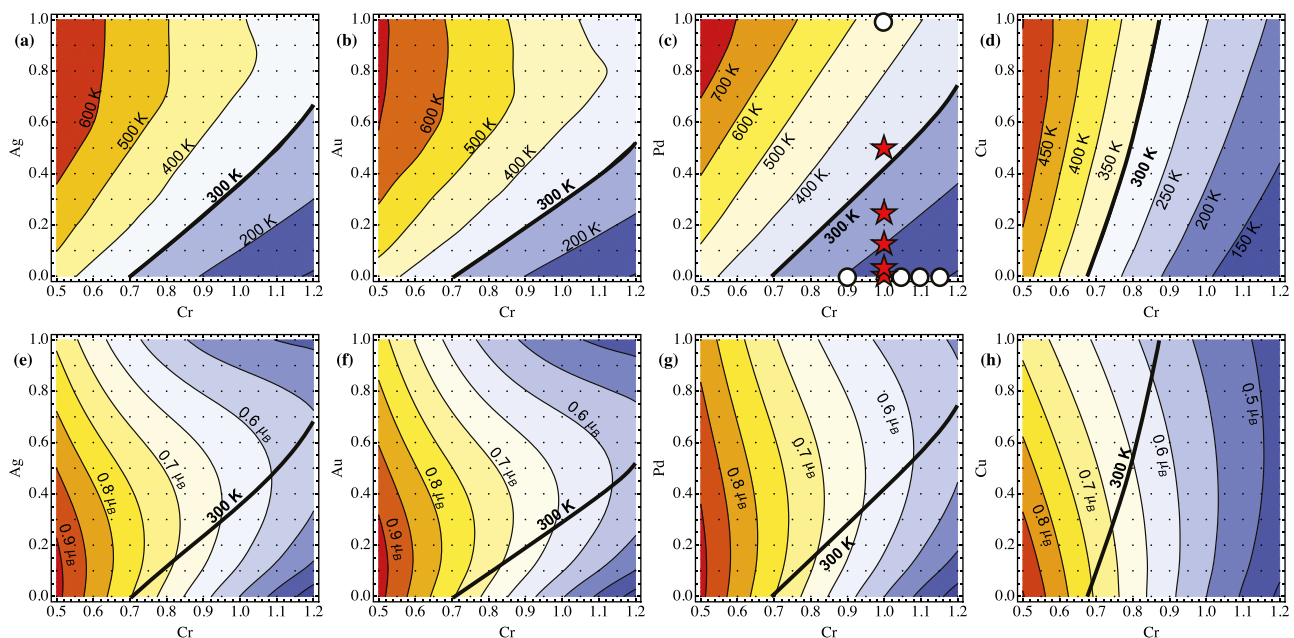


FIG. 3. Upper row (a)–(d): Curie temperature maps for CoCrFeNi-based alloys. The x- and y-axis define the Cr- and (Ag,Au,Cu,Pd)-content. Thick lines indicate compositions where T_C 's close to room temperature are predicted. Markers indicate previous experimentally explored compositions (black circles) as well as our measurements (red stars), see also Fig. 2 for comparison. Lower row (e)–(h): The corresponding saturation magnetization at $T=0$ K per site.

temperature should be the Curie point; these are summarized in Table I.

Magnetic refrigeration applications require not only T_C near room temperature but also as high as possible saturation magnetization. In parallel to the T_C computations, we have explored saturation magnetization maps for all considered alloys. As shown in Fig. 3 (lower row), the magnetization is not significantly different using the different FCC additions. One might expect that increasing the equilibrium volume via alloying should in principle increase the magnetization. The reason why this is not prominently observed is that the increase in local moments of the ferromagnetic constitutions Co, Fe, and Ni with increasing volume is partially compensated by the steeper increase of the anti-ferromagnetic aligned Cr moments. Of course, alloying with Ag, Au, Pd, and Cu also decreases the net magnetization because of dilution of the ferromagnetic components Fe, Co, and Ni. For all considered systems, the largest saturation magnetization values are found for the smallest Cr-concentrations which is again directly related to the anti-ferromagnetic alignment of Cr-atoms at $T=0$ K. The theoretical predictions for Pd addition are also in qualitative agreement with our own measurements. The provided T_C and magnetization maps can be used as a guide to adjust and fine-tune the alloy compositions to a target T_C and magnetization.

While the agreement with experiment will make this work impactful, our theoretical predictions are limited by the lack of sophisticated stability analysis tools. Empirical rules that were previously applied to determine HEA stabilities³⁹ are presently being replaced by first-principles approaches⁴⁰ that reveal new and unexpected tendencies. So far, however, these first principles approaches consider only $T=0$ K energetics, and a fully theory-guided finite T approach has yet to be developed within the community.

In summary, we presented a combined mean field and density-functional theory study to compute Curie temperatures of high entropy alloys. Our results are in excellent agreement with available experimental data for a number of different HEAs, including subtle concentration dependent trends. In addition to the previously experimentally identified alloying strategies to achieve room temperature ferromagnetism in CoCrFeNi alloys, we suggest three more alternative alloying candidates, namely, Ag, Au, and Cu, each of which has a variety of compositions that should exhibit room temperature ferromagnetism. Room temperature T_C 's are predicted by approximate linear relations for the stoichiometric compositions between Cr and alloying elements Ag, Au, Cu, and Pd (Table I). We thus reveal a large set of candidate materials, such as CoFeNiCrAg_{0.37}, CoFeNiCrAu_{0.29}, or

CoFeNiCr_{0.8}Cu_{0.64}. The theoretical T_C maps can be directly applied to create ferromagnetic HEAs with well-defined target T_C 's and magnetizations.

The authors would like to express their sincere gratitude to Professor Andrei V. Ruban at Royal Institute of Technology, Stockholm, Sweden for fruitful discussions on the EMTO calculations. Funding by the European Research Council under the EU's 7th Framework Programme (FP7/2007-2013)/ERC Grant Agreement No. 290998 and by the Deutsche Forschungsgemeinschaft (DFG) for the scholarship KO 5080/1-1 are gratefully acknowledged. Work at USF and RIT was supported by the U.S. National Science Foundation through Award No. 1522927; we thank J. Horwath for discussions.

- ¹B. Murty, J.-W. Yeh, and S. Ranganathan, *High-Entropy Alloys* (Butterworth-Heinemann, 2014); Y. Zhang, T. T. Zuo, Z. Tang, M. C. Gao, K. A. Dahmen, P. K. Liaw, and Z. P. Lu, *Prog. Mater. Sci.* **61**, 1 (2014).
- ²B. Gludovatz, A. Hohenwarter, D. Catoor, E. H. Chang, E. P. George, and R. O. Ritchie, *Science* **345**, 1153 (2014).
- ³M. S. Lucas, L. Mauger, J. A. Muñoz, Y. Xiao, A. O. Sheets, S. L. Semiatin, J. Horwath, and Z. Turgut, *J. Appl. Phys.* **109**, 07E307 (2011).
- ⁴M. S. Lucas, D. Belyea, C. Bauer, N. Bryant, E. Michel, Z. Turgut, S. O. Leontsev, J. Horwath, S. L. Semiatin, M. E. McHenry *et al.*, *J. Appl. Phys.* **113**, 17A923 (2013).
- ⁵O. Tegus, E. Brück, K. H. J. Buschow, and F. R. de Boer, *Nature* **415**, 150 (2002); K. G. Sandeman, *Scr. Mater.* **67**, 566 (2012); H. Ucar, J. J. Ipus, V. Franco, M. E. McHenry, and D. E. Laughlin, *JOM* **64**, 782 (2012); O. Gutflisch, M. A. Willard, E. Brück, C. H. Chen, S. G. Sankar, and J. P. Liu, *Adv. Mater.* **23**, 821 (2011); R. D. McMichael, R. D. Shull, L. J. Swartzendruber, L. H. Bennett, and R. E. Watson, *J. Magn. Magn. Mater.* **111**, 29 (1992).
- ⁶Y.-F. Kao, S.-K. Chen, T.-J. Chen, P.-C. Chu, J.-W. Yeh, and S.-J. Lin, *J. Alloys Compd.* **509**, 1607 (2011).
- ⁷G. Y. Gao, K. L. Yao, E. Şaşıoğlu, L. M. Sandratskii, Z. L. Liu, and J. L. Jiang, *Phys. Rev. B* **75**, 174442 (2007).
- ⁸M. Pajda, J. Kudrnovsky, I. Turek, V. Drchal, and P. Bruno, *Phys. Rev. B* **64**, 174402 (2001).
- ⁹F. Körmann, A. Dick, B. Grabowski, B. Hallstedt, T. Hickel, and J. Neugebauer, *Phys. Rev. B* **78**, 033102 (2008).
- ¹⁰F. Körmann, A. Dick, T. Hickel, and J. Neugebauer, *Phys. Rev. B* **79**, 184406 (2009).
- ¹¹M. Ležaić, P. Mavropoulos, and S. Blügel, *Appl. Phys. Lett.* **90**, 082504 (2007).
- ¹²A. V. Ruban, S. Khmelevskiy, P. Mohn, and B. Johansson, *Phys. Rev. B* **75**, 054402 (2007).
- ¹³F. Körmann, A. Dick, T. Hickel, and J. Neugebauer, *Phys. Rev. B* **81**, 134425 (2010).
- ¹⁴N. M. Rosengaard and B. Johansson, *Phys. Rev. B* **55**, 14975 (1997).
- ¹⁵F. Körmann, A. A. H. Breidi, S. L. Dudarev, N. Dupin, G. Ghosh, T. Hickel, P. Korzhavyi, J. A. Muñoz, and I. Ohnuma, *Phys. Status Solidi B* **251**, 53 (2014); F. Körmann, T. Hickel, and J. Neugebauer, "Influence of magnetic excitations on the phase stability of metals and steels," *Curr. Opin. Solid State Mater. Sci.* (published online).
- ¹⁶E. Şaşıoğlu, L. M. Sandratskii, and P. Bruno, *Phys. Rev. B* **70**, 024427 (2004); **71**, 214412 (2005).
- ¹⁷K. Sato, P. Dederichs, and H. Katayama-Yoshida, *Europhys. Lett.* **61**, 403 (2003).
- ¹⁸G. Bouzerar, J. Kudrnovsky, L. Bergqvist, and P. Bruno, *Phys. Rev. B* **68**, 081203 (2003).
- ¹⁹L. Bergqvist, O. Eriksson, J. Kudrnovský, V. Drchal, P. Korzhavyi, and I. Turek, *Phys. Rev. Lett.* **93**, 137202 (2004).
- ²⁰L. Bergqvist, B. Belhadji, S. Picozzi, and P. H. Dederichs, *Phys. Rev. B* **77**, 014418 (2008).
- ²¹K. Sato, L. Bergqvist, J. Kudrnovský, P. H. Dederichs, O. Eriksson, I. Turek, B. Sanyal, G. Bouzerar, H. Katayama-Yoshida, V. Dinh *et al.*, *Rev. Mod. Phys.* **82**, 1633 (2010).
- ²²J. M. MacLaren, T. C. Schulthess, W. H. Butler, R. S. Sutton, and M. McHenry, *J. Appl. Phys.* **85**, 4833 (1999).

TABLE I. Predicted stoichiometric compositions revealing room temperature T_C CoFeNi-based HEAs.

| CoFeNiCr _x Q _y | $T_C = 300$ K ^a | Examples for CoFeNi+ |
|--------------------------------------|----------------------------|---|
| Q = Cu | $y \approx -4.69 + 6.67x$ | CrCu _{1.97} , Cr _{0.8} Cu _{0.64} |
| Q = Pd | $y \approx -1.02 + 1.45x$ | CrPd _{0.43} , Cr _{1.2} Pd _{0.72} |
| Q = Ag | $y \approx -0.93 + 1.30x$ | CrAg _{0.37} , Cr _{1.2} Ag _{0.63} |
| Q = Au | $y \approx -0.74 + 1.03x$ | CrAu _{0.29} , Cr _{1.2} Au _{0.50} |

^aFrom least square fit to the computed data.

- ²³K. Sato, W. Schweika, P. Dederichs, and H. Katayama-Yoshida, *Phys. Rev. B* **70**, 201202 (2004).
- ²⁴L. Vitos, *Phys. Rev. B* **64**, 014107 (2001); A. V. Ruban and H. L. Skriver, *ibid.* **66**, 024201 (2002); A. V. Ruban, A. B. Belonoshko, and N. V. Skorodumova, *ibid.* **87**, 014405 (2013); M. Rahaman, B. Johansson, and A. V. Ruban, *ibid.* **89**, 064103 (2014); L. Vitos, H. L. Skriver, B. Johansson, and J. Kollár, *Comput. Mater. Sci.* **18**, 24 (2000); L. Vitos, *Computational Quantum Mechanics for Materials Engineers: The EMTO Method and Applications* (Springer Science & Business Media, 2007).
- ²⁵J. P. Perdew, K. Burke, and M. Ernzerhof, *Phys. Rev. Lett.* **77**, 3865 (1996); Self-consistent electronic density calculations employ the local density approximation, while the total energy has been obtained within the GGA.
- ²⁶P. Soven, *Phys. Rev.* **156**, 809 (1967); B. L. Gyorffy, *Phys. Rev. B* **5**, 2382 (1972).
- ²⁷J. Staunton, B. L. Gyorffy, A. J. Pindor, G. M. Stocks, and H. Winter, *J. Magn. Magn. Mater.* **45**, 15 (1984); B. L. Gyorffy, A. J. Pindor, J. Staunton, G. M. Stocks, and H. Winter, *J. Phys. F: Met. Phys.* **15**, 1337 (1985).
- ²⁸F. Tian, L. Delczeg, N. Chen, L. K. Varga, J. Shen, and L. Vitos, *Phys. Rev. B* **88**, 085128 (2013).
- ²⁹F. Tian, L. K. Varga, N. Chen, L. Delczeg, and L. Vitos, *Phys. Rev. B* **87**, 075144 (2013).
- ³⁰F. Tian, L. K. Varga, N. Chen, J. Shen, and L. Vitos, *J. Alloys Compd.* **599**, 19 (2014).
- ³¹E. Fazakas, V. Zadorozhnyy, L. K. Varga, A. Inoue, D. V. Louzguine-Luzgin, F. Tian, and L. Vitos, *Int. J. Refract. Met. Hard Mater.* **47**, 131 (2014).
- ³²P. Cao, X. Ni, F. Tian, L. K. Varga, and L. Vitos, *J. Phys.: Condens. Matter* **27**, 075401 (2015).
- ³³D. Ma, B. Grabowski, F. Körmann, J. Neugebauer, and D. Raabe, *Acta Mater.* **100**, 90 (2015).
- ³⁴C. Niu, A. J. Zaddach, A. A. Oni, X. Sang, J. W. Hurt III, J. M. LeBeau, C. C. Koch, and D. L. Irving, *Appl. Phys. Lett.* **106**, 161906 (2015).
- ³⁵A. J. Zaddach, C. C. Niu, C. Koch, and D. L. Irving, *JOM* **65**, 1780 (2013).
- ³⁶S. Huang, W. Li, S. Lu, F. Tian, J. Shen, E. Holmström, and L. Vitos, *Scr. Mater.* **108**, 44 (2015).
- ³⁷H. J. Monkhorst and J. D. Pack, *Phys. Rev. B* **13**, 5188 (1976).
- ³⁸A. Arrott and J. E. Noakes, *Phys. Rev. Lett.* **19**, 786 (1967).
- ³⁹Y. Zhang, Y. J. Zhou, J. P. Lin, G. L. Chen, and P. K. Liaw, *Adv. Eng. Mater.* **10**, 534 (2008).
- ⁴⁰M. C. Tropaevsky, J. R. Morris, P. R. C. Kent, A. R. Lupini, and G. M. Stocks, *Phys. Rev. X* **5**, 011041 (2015).